Crawford, A. O., Cavalli, G., Howlin, B. J., & Hamerton, I. (2016). Investigation of structure property relationships in liquid processible, solvent free, thermally stable bismaleimide-triazine (BT) resins. *Reactive and Functional Polymers*, *102*, 110-118. https://doi.org/10.1016/j.reactfunctpolym.2016.03.002

Investigation of structure property relationships in liquid processible, solvent free, thermally stable Bismaleimide-Triazine (BT) resins

Alasdair O. Crawford[1], Gabriel Cavalli[2], Brendan J. Howlin[2], Ian Hamerton[3,*]

[1]Henkel Ltd., 957 Buckingham Avenue, Slough, SL1 4NL, U.K.

[2]Department of Chemistry, Faculty of Engineering and Physical Sciences, University of Surrey, Guildford, Surrey, GU2 7XH, U.K.

[3]The Advanced Composites Centre for Innovation and Science, Department of Aerospace Engineering, Queen's Building, University of Bristol, Bristol, BS8 1TR, U.K.

[*] *Correspondence to Dr Ian Hamerton, The Advanced Composites Centre for Innovation and Science, Department of Aerospace Engineering, Queen's Building, University of Bristol, Bristol, BS8 1TR, U.K. E-mail: ian.hamerton@bristol.ac.uk*

ABSTRACT: Three cyanate ester monomer or oligomer species: 2,2-bis(4-cyanatophenyl)propane **1**, 1-1-bis(4-cyanatophenyl)ethane (2), and the oligomeric phenolic cyanate (Primaset^{TM} PT30) (3), are blended in various ratios with bis(4-maleimidophenyl)methane, (4), to form binary and ternary mixtures (11 in total) and cured, in the absence of catalysts (3 K/min to 150 °C + 1 hour; 3 K/min to 200 °C + 3 hours), followed by a post cure (3 K/min to 260 °C + 1 hour). The use of liquid monomer, (2), offers the possibility of liquid processing in blends containing minority compositions of bismaleimide. Glycidylmethacrylate is explored as a reactive diluent (2.5-10 wt %) to linked interpenetrating network polymer structures comprising cyanate ester and bismaleimide components with glass transition temperatures of 267-275 ºC, depending on composition; the onset of thermo-oxidative degradation ranges from 386-397 ºC. When a binary blend of (2) and (3) (with the former in the minority) is co-cured with (4), an excellent balance of properties is achieved with liquid processing, a T_g greater than 400 °C and onset of degradation of 425 ºC in static air. Kinetic analysis of DSC data using Ozawa and Kissinger methods yield activation energies of between 107-112 kJ/mole for a binary blend of $(1)_{90}$-$(4)_{10}$, which is in good agreement with literature. Molecular dynamics simulation of the same blend in cured form gave a simulated glass transition temperature of 250 °C that is in very close agreement with empirical DMTA data.

Keywords: Cyanate Esters, Bismaleimide-triazine resins, Polymerisation kinetics, Thermal analysis, thermo-oxidative stability, molecular modelling.

INTRODUCTION

Cyanate esters (CEs) constitute a family of addition cured high performance, thermosetting polymers, which occupy a niche intermediate between high glass transition temperature (T_g), tetrafunctional epoxy resins and bismaleimides (BMIs) [1]. Cured CEs offer a combination of favourable thermal and mechanical performance (*e.g.* dry T_g values of 270-300 °C are common with a strain at break of over 5-8 %) that gives a unique property profile. Although requiring toughening for some engineering applications, cyanates can be combined with inherently tough engineering thermoplastics (HexPly 954-2A, G_{IC} = 250 J/m^2) [2,3] or elastomers (HexPly 953-3, G_{IC} = 450 J/m^2) [4] to yield impressive enhancements. In this form they typically find application as matrices in advanced composites (either in combination with epoxy resins in aerospace applications [5,6]). The low loss properties and microwave transparency makes CE resins of particular interest in the fabrication of radomes (*e.g.* Augusta Westland Helicopter's AW101 Merlin uses a Kevlar^{TM}/CE sandwich bonded skin [8]), where a material with high dielectric constant or dissipation factor would otherwise result in attenuation of signal along with the structure of the radome itself being heated through conversion of electromagnetic energy to thermal energy. The typical material of a radome will be exposed to frequencies in the region of 600 MHz to 100 GHz and should have dielectric constants (D_k) of less than 3 and dissipation factors (D_f) of less than 0.010 [1]. Along with the electrical properties integral to signal transduction, the material used for radome construction must possess both thermal and mechanical properties capable of withstanding the environment required. The nosecones of aircraft, missile tracking noses, and weather radar all require resistance to high temperatures, whilst maintaining their electrical properties [7]. This aspect is not examined in this paper, but will be addressed with the subsequent analysis of glass fibre reinforced composites utilising these matrices.

CEs are combined with BMIs as dielectric polymers in the microelectronics industry [9], a business which is predicted to be reach a value of some $94 billion by 2017 [10]. This was the first application of CE resins and still represents the largest market share by application, taking advantage of their excellent electrical properties. A particularly well-established material in this area is the family of bismaleimide-triazine (BT) resins which is made up of multicomponent blends produced by Mitsubishi Gas Chemical Co. comprising a BMI [11] and a CE combined with high boiling organic solvents, to facilitate processing. BT resins were first marketed in 1978 [12] incorporating methylene dianiline and triazine A (a cyanate oligomer based on bisphenol A) and initially found wide application in printed circuit boards. With the advancement in these technologies since the late 1970s and the subsequent increase in the number and complexity of electronic devices (coupled with increasing miniaturisation) has led to greater demand for CEs in this field. The combination of low dielectric constant and low loss properties and reduced 'cross

talk', make these materials particularly attractive in multilayer chip modules [13]. As the thickness of circuit boards increases due to layering of circuitry, the dielectric properties of the polymeric material becomes more important, ensuring optimal signal propagation whilst remaining thermally and mechanically reliable. This is also true for multichip modules synthesised through film deposition and film lamination, where thin layer conductors are insulated by a thin film of CE hybrid [14].

The approach taken in this work has been to build on the undoubted attractions of the BT resins, while addressing the shortcomings in the standard BT resin chemistry: achievement of a single T_g through linking the polymer domains in the network structure; reducing the reliance on high boiling organic solvents and improving processability by introducing a reactive diluent or improving thermal and dimensional stability.

EXPERIMENTAL

Instrumentation.

Differential scanning calorimetry (DSC) was undertaken using a TA Instruments Q1000 running TA Q Series Advantage software on samples (5.0 ± 0.5 mg) in hermetically sealed aluminium pans. Experiments were conducted at a heating rate of 10 $Kmin^{-1}$. from -10 °C to 400 °C (heat/cool/heat) under flowing nitrogen (50 cm^3/min.).

Thermogravimetric analysis (TGA) was performed on a TA Q500 on milled, cured resin samples (6.5 ± 0.5 mg) in a platinum crucible from 20-800 °C at 10 $Kmin^{-1}$ in air and nitrogen (40 cm^3/min).

Dynamic mechanical thermal analysis (DMTA) (in single cantilever mode at a frequency of 1 Hz) was carried out on cured neat resin samples (*ca.* 3 × 5 × 17 mm^3) using a TA Q800 in static air from 20 °C to 400 °C at 3 $Kmin^{-1}$ at 0.1 % strain.

Materials. The dicyanate ester monomers: 2,2-bis(4-cyanatophenyl)propane (1**)**, 1,1-bis(4-cyanatophenyl)ethane (2), and the oligomeric phenolic cyanate (average value of n =1) (3), were all supplied by Lonza Ltd (Visp, Switzerland), 4,4-bis(4-maleimideophenyl)methane (95%), (4) was obtained from Sigma Aldrich, glycidylmethacrylate, GMA (5), was provided by Dow Chemical. All monomers were characterised fully using spectroscopic (^{1}H NMR, Raman), elemental and thermal analysis and used as received without further purification.

Scheme 1 Monomer structures studied in this work (*N.B.,* in this instance n = 1 in structure (3))

Blending and cure of polymer samples. The blended monomeric components were decanted into aluminium dishes (55 mm diameter, depth 10 mm) cured in a fan-assisted oven heating at 3 $Kmin^{-1}$

to 160 °C (1 hour isothermal) + heating at 3 $Kmin^{-1}$ to 200 °C (3 hours isothermal) then post cured - heating at 3 $Kmin^{-1}$ to 260 °C (1 hour isothermal) followed by a gradual cool (3 $Kmin^{-1}$) to room temperature. Cured samples of the different blends (Table 1) were cut to correct size for analysis. Where glycidyl methacrylate, (5), was incorporated, the blends were prepared by heating the mixture of monomers with/without GMA to *ca.* 100 °C to melt the solid cyanate ester component, where they were then mixed with a magnetic stirrer (300 rpm, 10 minutes). A typical mixture for replicate DMTA analyses might comprise 10 g, so the blend $(1)_{90}$-$(4)_{10}$, denoted the 'standard' BT resin, contained cyanate monomer (1) (9 g, 3.23 x 10^{-2} mole) and BMI (4) (1 g, 2.79 x 10^{-3} mole). The homogenous mixture was placed in an oven, ramping from 100 °C to 160 °C at 3 $Kmin^{-1}$, before following the cure schedule: 160 °C (1 hour isothermal), ramp at 3 $Kmin^{-1}$ then 200 °C (3 hours isothermal, ramp at 3 $Kmin^{-1}$ to 260 °C (1 hour isothermal post cure).

Table 1 Designation of monomers and blends examined in this work

THEORY

Molecular simulation. Modelling was performed using Materials Studio v. 5.5.0.0 (Accelrys™, 2010) on a Dell PC (Optiplex™ 780, Intel Core Duo 3.00 GHz, 4.00 GB RAM, 100 GB HDD). Potential energies were calculated using the Polymer Consistent Force Field (PCFF) [15]. When modelling blends of Primaset™ PT30, the Legacy module within Materials Studio was used to construct an amorphous cell with 49 PT30 oligomers (n = 1) with corresponding numbers of either 2,2-bis(4-cyanatophenyl)propane or 1-1-bis(4-cyanatophenyl)ethane monomers to make up the correct stoichiometry of the blend. The distribution of *ortho*- and *para*-substituted phenyl rings was chosen based on data from empirical ^{13}C NMR studies carried out on the phenolic precursor and compared with previous work [16,17]: *ortho-ortho* (22 %), *ortho-para* (56 %), and *para-para* (22 %) substitutions. The target density for the cell was set at 1.25 gcm^{-3}, consistent with experiment [18] and previous simulations [19]. The resulting amorphous cells comprised 3580-6224 atoms.

The cyanate groups were bonded manually to form 1,3,5-triazine rings and a minimization of 500 iterations was carried out to relieve the strain using the Discover minimization module to a convergence of 1000 $kcalmol^{-1}Å^{-1}$. A conjugate gradients minimization was then carried out to a convergence of 100 $kcalmol^{-1}Å^{-1}$. Bonds were reacted through the faces of the unit cell to neighbouring periodic boxes to simulate an infinite 3–D cross-linked network. A total of 138 out of the 147 functional groups were co-reacted, corresponding to a monomer conversion of 94 %, which is typical for this type of polymer [20]. After the final cyclotrimerization the system was submitted to a final minimization of 10,000 iterations.

Equilibration was undertaken using a 1 ns molecular dynamics (MD) simulation (25 °C) using the Discover single run option. An isothermal–isobaric ensemble, wherein the number of atoms (N), pressure (P) and temperature (T) are conserved, was used with a time step of 1 fs; the Anderson thermostat was combined with the Berendsen Barostat [21]. PCFF was used with the atomic van der Waals summation, a cut-off of 10.00 Å, a spline width of 3.00 Å and a buffer width of 1.00 Å. The system was subjected to a second 10 ps MD simulation at 500 °C using the same parameters as above to equilibrate the system for the upper temperature of the temperature ramped MD simulations (the latter were performed using the Temperature Cycle option in the Legacy Protocols module). 51 MD simulations were run between 500 °C and 0 °C in decrements of 10 K; at each temperature stage a 125 ps MD simulation was carried out. The first 25 ps of each simulation were used to equilibrate the system and the subsequent 100 ps simulation was used to record the results. A plot of calculated cell density was plotted against simulation temperature to determine both the T_g and the degradation onset temperature.

RESULTS AND DISCUSSION

Commercially manufactured BT resin usually contains several high boiling solvents [22], which can present some potential hazards to users and the environment during processing and disposal. Several approaches were taken in this work to explore alternatives to reducing the reliance on solvents and incidentally co-catalysts. Initially, a short study was conducted to examine the conditions under which the BMI, (4), might be blended with the liquid dicyanate ester, based on bisphenol E, (2) to form a stable miscible liquid. Thus, seven blends of $(2)_{90}$-$(4)_{10}$ were investigated through different dissolution methods (Table 2) and the results are illustrated (Fig. 1, See Supplementary Fig. S1 for colour image). A range of solvated blends is displayed from comparatively clear, to slightly turbid liquids, but the fluidity of the blends is self evident.

Fig. 1 Samples A-D (left to right). Note the treatment of samples E-G did not effect dissolution.

It was felt that adopting the use of a liquid monomer as a solvent matrix might enable the solvation of the solid BMI component facilitating industrial processing methods. This was explored with both (2), a liquid monomer based on bisphenol E dicyanate, and (3) (PT30), an oligomeric cyanate ester. Finally, the best performing binary CE blend, $(3)_{90}$-$(2)_{10}$ was blended with BMI, (4). In previous work [21], the binary blend $(3)_{90}$-$(2)_{10}$ has shown significant reduction in outgassing, combined with good thermal and mechanical properties. Several processing procedures (Table 2) were examined, with varying levels of success. While the blends or conditions did not produce

entirely homogenous blends, it is evident that sonication (Fig. 1, B-D) demonstrates there is a clear possibility of using (2) as a solvent or to aid dispersion of the BMI component in a novel BT resin.

Table 2 Conditions applied to aid co-solvation of (2) and (4).

Determination of thermal polymerisation behaviour of interpenetrating networks. DSC analysis was performed on uncured blends of $(1)_{90}$-$(4)_{10}$, $(2)_{90}$-$(4)_{10}$, $(3)_{90}$-$(4)_{10}$ and $(3{:}2)_{90:10}$-$(4)_{10}$ to assess any differences in the onset of polymerisation and the overall enthalpy of the polymerisation, these data are summarised in Fig. 2 and Table 3.

Table 3 DSC data for uncured novel bismaleimide-triazine blends (nitrogen, 10 K/minute)

The thermogram for the 'standard' BT resin $(1)_{90}$-$(4)_{10}$ shows a clear endotherm (T_m = 80 °C) from the dicyanate component, whereas the remaining blends are liquid at room temperature. From the raw thermal data obtained from dynamic DSC (Fig. 2), there appears to be little difference in the onset of the thermal polymerisation, although the cure moves into a lower temperature regime (with both the T_{max} and conclusion of the polymerisation reactions move up to 30 K). The liquid (3) appears to enhance the reactivity to the greatest extent, particularly when combined with the more fluid monomer, (2).

Fig. 2 DSC analysis of $(1)_{90}$-$(4)_{10}$, $(2)_{90}$-$(4)_{10}$, $(3)_{90}$-$(4)_{10}$, and $(3{:}2)_{90:10}$-$(4)_{10}$.

Determination of thermal polymerisation kinetics. The data obtained from the DSC analyses was examined to determine the influence of the monomer blend on the thermal reactivity of the BT resins. In each case the DSC data were used to generate both a plot of apparent reaction rate and fractional conversion for the polymerisation reaction(s) (Figs 3-5), from which the enhanced reactivity of the blends containing CE (3) is immediately apparent, not only in terms of the peak of maximum reaction rate at 10 K/min ($(3{:}2)_{90:10}$-$(4)_{10}$, 0.08 s^{-1} *cf* $(1)_{90}$-$(4)_{10}$, 0.013 s^{-1}), but also crucially in terms of the conclusion of the bulk of the reaction, which takes place at a significantly lower temperature than the other blends tested, or the homopolymers.

Fig 3 Plots of (a) reaction rate and (b) fractional conversion data from DSC heating scan (various heating rates, under nitrogen) for $(1)_{90}$-$(4)_{10}$.

Fig 4 Plots of (a) reaction rate and (b) fractional conversion data from DSC heating scan (various heating rates, under nitrogen) for $(3)_{90}$-$(4)_{10}$.

Fig 5 Plots of (a) reaction rate and (b) fractional conversion data from DSC heating scan (various heating rates, under nitrogen) for $(3{:}2)_{90:10}$-$(4)_{10}$.

The activation energy for the polymerization processes were calculated using both the Kissinger (eqn 1) and Ozawa (eqn 2) methods and the regression coefficients (R^2 values) show reasonably linear fits to the DSC data, with the poorest fit, for $(1)_{90}$-$(4)_{10}$, being 0.94-0.95 (Fig. 6).

$$ln\frac{\beta}{T_p^{2^2}} = ln\left(\frac{Q_p AR}{E_a}\right) - \frac{E_a}{RT_p} \quad (1)$$

where $Q_p = -[df(\alpha)/d(\alpha)]_{\alpha=\alpha p}$, T_p is the maximum temperature of the exothermic peak, E_a = activation energy, R = Gas constant, and β is the heating rate employed.

$$ln\beta = ln\left(\frac{AE_a}{R}\right) - lnf(\alpha) - 5.331 - 1.052\left(\frac{E_a}{RT}\right) \quad (2)$$

where A = the Arrhenius pre-exponential factor and f is a constant function.

Fig. 6 Kinetic parameters from DSC heating scan (various heating rates, nitrogen) for $(1)_{90}$-$(4)_{10}$.

A similar analysis of the two blends containing CE (3) was performed and in both cases the R^2 values are very consistent > 0.99 (Figs. 7,8), showing extremely good agreement.

Fig. 7 Kinetic parameters from DSC (various heating rates, nitrogen) for $(3)_{90}$-$(4)_{10}$.

Fig. 8 Kinetic parameters from DSC (various heating rates, nitrogen) for $(3{:}2)_{90:10}$-$(4)_{10}$.

The resulting activation energies derived from the Ozawa and Kissinger calculations (Table 4) suggest an activation energy of 107-112 kJ/mole for the standard blend, $(1)_{90}$-$(4)_{10}$, which is higher than the activation energy for the corresponding homopolymers (80-120 kJ/mole cyanate [23,24,25]) or the binary cyanate blends (64-68 kJ/mole cyanate for $(1)_{50}$-$(2)_{50}$; 100-106 kJ/mole cyanate for $(3)_{50}$-$(1)_{50}$ and $(3)_{50}$-$(2)_{50}$, [22]), and in reasonable agreement with a previous report of a BT resins (91 kJ/mole) [26]. The asymmetrical nature of the polymerization exotherm, coupled with the changes in reaction rate through the exotherm, suggests a reaction mechanism that is complex, involving more than one step.

Table 4 Kinetic parameters (DSC data) for uncured novel bismaleimide-triazine blends

Whereas other researchers have reported [27,28,29,30] evidence of co-reaction in the presence of specific catalysts, there is no evidence for any unique structures. Previous work [22,31] has suggested that under the conditions used here (in the absence of catalyst) an interpenetrating network (IPN) is formed, with the two components of the blend undergoing homopolymerisation in the presence of one another, albeit more sluggishly than as homopolymers. For the blends involving CE (3), the application of both the Kissinger and Ozawa methods is more satisfactory (R^2 values > 0.99) show good, linear fits to the DSC data. The activation energy data for the $(3)_{90}$-$(4)_{10}$ blend exhibits an activation energy of between 93 and 98 kJ/mol cyanate which is lower than the original $(1)_{90}$-$(4)_{10}$ blend (107-112 kJ/mol cyanate) and more in line with reported values for other CE monomers. In the more complex blend, $(3{:}2)_{90:10}$-$(4)_{10}$, the data are still encouraging with an activation energy of 90-105 kJ/mol cyanate).

Examination of the thermo-oxidative stability of the cured BT blends.

A selection of the cured BT blends were analysed using TGA to determine their thermo-oxidative stability. Initially, the BMI homopolymer, [(4)], is by far the most stable of the polymers tested in this work, but there is a marked reversal in the stability of the polymer between 480-500 °C which is accompanied by a significant loss in mass (*ca.* 20-30 %). A second degradation step, resulting in a greater loss in mass, occurs above 500 °C.

Fig. 9 Thermo-oxidative stability of the cured BT resin blends (10 K/min, static air).

Table 5 Thermo-oxidative stability data (10 $Kmin^{-1}$, static air) for cured homopolymers and binary cyanate ester blends as determined by TGA

In previous work [32], the degradation mechanism of BMI homopolymers (and related citraconimides and nadimides) was examined under similar conditions (albeit at a lower heating rate, 2 $Kmin^{-1}$). Similar degradation profiles were observed (in terms of onset temperature and peak maxima) and char yields were equally low in air, *ca.* 1 %. In this work, all the blends display similar levels of thermo-oxidative stability, but once again $(3{:}2)_{90:10}$-$(4)_{10}$, combining two CE monomers is the most stable of the cured blends tested.

Examination of the thermal and thermomechanical properties of the cured BT blends.

Having established the relative reactivity of the blends, the thermo-mechanical properties of the blends were investigated to assess for whether there was any clear advantage in producing a BT resin with the phenolic oligomeric cyanate moiety. PT30 outperforms bisphenol A dicyanate in thermo-mechanical testing (in terms of modulus and T_g), it was hypothesised that the resulting blend between (3) and BMI, (4) might outperform the blend between (1) and (4). Consequently, a series of blends was prepared containing various quantities of CE and BMI. The thermally cured plaques were homogenous and void free in all cases although increasing the BMI content led to an increased brittleness in the cured material, although this tendency toward fracture was also observed with the BT blends containing (1) and (4), making *e.g.* the blend containing equal quantities of both component, $(1)_{50}$-$(4)_{50}$, particularly difficult to analyse using DMTA. A comparison of the storage moduli from DMTA (Fig. 10) demonstrates the potential advantage of combining the oilgomeric phenolic CE, (3), with the BMI rather than the bisphenyl type structures through the enhanced thermo-mechanical properties. The data for $[(1)_{90}$-$(4)_{10}]$ displays a lower modulus (at least 500 MPa) and lower T_g (*ca.* 230 °C) compared with the same blend composition $[(3)_{90}$-$(4)_{10}]$. The latter maintains a high degree of thermo-mechanical integrity, with storage modulus exhibiting a gradual decline up to the T_g at 380 °C at which point the experiment was terminated due to the upper temperature limit of the instrument's furnace being reached.

Fig. 10 Comparison of DMTA data for selected cured polycyanurate-BMI blends.

While it was difficult to determine the T_g of some of the more highly aromatic and highly crosslinked systems, was informative to determine the storage modulus of the cured polymers near room temperature and at elevated temperature, 300 °C (Table 5.9).

Table 6 Storage moduli (DMTA) for cured homopolymers and blends.

Modelling the thermomechanical behaviour of the $[(1)_{90}$-$(4)_{10}]$ blend

Previous research has concentrated on modeling CE homopolymers [33] and binary blends [34] and their physical properties, which, while complex, were conceptually comparatively simple as both components were co-reactive. In the present work, the simulation of a BT type resin requires that the CE matrix (in the majority) contains a small but discrete quantity of BMI. The preliminary data obtained [22] through investigation was comprehensive and enabled a representative model for a BT resin for the first time. The crucial piece of information that is key to the successful modelling of a BT resin is an understanding of the reaction mechanism and the polymeric network produced. As the network produced between CE and BMI in the absence of catalyst is an interpenetrating

network a modelling technique could be established ensuring that monomeric units only reacted with their identical monomeric counterparts to yield homopolymers rather than co-reacting, thus creating an IPN. The models were produced in an identical methodology as had been done for the molecular modelling of the binary cyanates with one notable modification to the technique. The effect of the increased dynamics time discussed in the methodology is shown clearly (Fig. 11), with the system becoming fully equilibrated after 1 ns.

Fig. 11 MD temperature equilibration over (a) 10000 fs (10 ps), (b) 1 ns.

This increase in molecular dynamics duration was required to produce accurate calculations of T_g. It is clear in Fig. 11a that the model is not fully equilibrated at the elevated temperature of the molecular dynamics simulation and it is the potential energy of the system that requires a longer time step. The fully equilibrated model is shown by Fig. 11b. This increase in dynamics duration required considerably more time and computing power to complete than the binary cyanate ester blends. However, the resultant data produced from these MD calculations are of high quality and demonstrate the possibility of modelling BT style resin systems. The data produced, shown in Fig. 12, demonstrate a clear T_g of 250 °C in the blend (the empirical data derived from DMTA experiment are shown in the same figure).

Fig. 12. MD density data for $[(1)_{90}\text{-}(4)_{10}]$ superimposed on loss modulus data (single cantilever, K/min, under nitrogen)

There is always a trade-off between simulation accuracy and time/computing power requirements by the user. In this case, this BT system required a significantly longer dynamics stage than the binary CE blends and would properly come into its own with access to greater computing power.

Examination of novel linked interpenetrating networks (LIPNs). A second liquid chemical linker (glycidyl methacrylate, GMA, (5)) was also investigated to assess whether incorporation of a linking unit between CE and BMI groups would facilitate the production of blended systems that would undergo a co-reactions to form an LIPN. Previous studies in this area have concentrated on diallyl functional dicyanate monomers [35,36], propenyl functional dicyanate monomers [37], and cyanate/propenyl modifiers [38] as a means to co-react the CE and BMI components. In each case, while the materials effected co-reaction and yielded polymer networks with attractive physical and mechanical properties, the preparative chemistry required at least several steps. In the present study, the choice of GMA was made on the basis of its dual chemical functionality and commercial

availability. It was anticipated that the methacrylic group would undergo reaction with the unsaturated BMI ring as this is well known [39], whilst the epoxide group (oxirane ring) would follow a more complex mechanism *via* the formation of oxazolidinone and oxazoline rings [40].

The quantity of GMA incorporated clearly would have an influence on a number of properties including T_g and moisture uptake. This is due to there being reduced cross-link density of the cured material if linear linking groups like GMA are introduced. This was examined in a previous study [41] through the combination of CEs with different acrylate monomers, *e.g.* butyl acrylate. Therefore, the amount of GMA requires optimisation to ensure that the thermal, mechanical and low moisture uptake properties of these materials are not jeopardised. Consequently, various quantities of GMA (2.5 wt %, 5 wt % and 10 wt %) were incorporated into the aforementioned 'standard' BT resin system $(1)_{90}$-$(4)_{10}$ (Table 7) Following a standard cure cycle (used previously in this work), it was immediately evident that with incorporation of GMA the plaques produced were homogenous. However, while the processing characteristics of the blend were good, they did not surpass the liquid processability of the tertiary blend $(3{:}2)_{90:10}$-$(4)_{10}$. Furthermore, even comparatively small amounts of GMA led to a significant reduction in thermo-oxidative stability

Table 7 Effect of GMA on thermo-mechanical performance of selected blends and LIPNs

(T_d), but still more markedly in T_g, which fell some 20 K on the addition of GMA (10 wt %). While the materials were not tested specifically for fracture toughness, there was some evidence of toughening in the systems containing higher GMA content, although the penalty in thermo-mechanical properties was deemed too great to continue with these materials within this project (although we shall return to examine these further in the future).

CONCLUSIONS

The aim of this project was to explore the possibility of producing a viable alternative to the market-leading bismaleimide-triazine (BT) resin, by concentrating on producing similar (or superior) thermo-mechanical properties, but enhancing the processability of the material by reducing the reliance on high boiling, environmentally harmful organic solvents. While the inclusion of glycidyl methacrylate offers some limited benefit as a reactive modifier, and there is some anecdotal evidence that toughness may be enhanced, the penalty in thermo-oxidative and dimensional stability was felt to be too high to pursue in this context. On the other hand, when the solid CE monomer, 2,2-bis(4-cyanatophenyl)propane (1), was replaced with a liquid CE monomer, 1-1-bis(4-cyanatophenyl)ethane (2), significant improvements in processing were obtained with

good solvation of the otherwise crystalline and high melting BMI monomer, bis(4-maleimidophenyl)methane, (4), following stirring and sonication. At the same time, given the structural similarity between (1) and (2), the reactivity of the BT blend was not appreciably improved. However, when the liquid oligomeric phenolic cyanate (Primaset^{TM} PT30) (3), was employed not only was blending much improved, but the blend became significantly more reactive. Still more impressive was the combination of a binary blend of (2) and (3) (with the former in the minority), which achieved a balance of improved (liquid) processing, the highest thermo-oxidative stability of the samples tested and T_g approaching 400 °C. In earlier studies, this binary blend of CE monomers reduced outgassing (usually caused by the production of carbamate species and subsequent decarboxylation at elevated temperatures greater than 200 °C) over CE hompolymers.

ACKNOWLEDGEMENTS.

We thank Lonza AG for funding this work, supporting AOC (research contract RD1107) and for supplying the cyanate monomers and Dr John Everett (Dow Chemical) for supplying the glycidylmethacrylate. The authors thank Drs Stefan Ellinger and Gaetano La Delfa (Lonza AG, Visp, Switzerland) for productive discussions during the course of the work and preparation of this manuscript.

REFERENCES

(1) *Chemistry and Technology of Cyanate Ester Resins*, Hamerton, I. (Ed.), Blackie A&P; Glasgow, **1994**.

(2) Tao, Q.S.; Gan, W.J.; Yue, Y.F.; Wang, M.H.; Tang, X.L.; Li, S.J. *Polymer*, **2004**, *45*, 3505-3510.

(3) Suman, J.; Kathi, J.; Tammishetti, S. *Euro. Polym. J.*, **2005**, *41*, 2963-2972.

(4) Nair, C.P.R.; Mathew, D.; Ninan, K. *Cyanate Ester Resins, Recent Developments, New Polymerisation Techniques and Synthetic Methodologies*, **2001**, Springer: Berlin, pp. 1-99.

(5) Karad, S.K.; Attwood, D.; Jones, F.R. *Composites Part A*, **2002**, *33*, 1665-1675.

(6) Leach, D.; Boyd, J. *Proc. 46th Int. SAMPE Symp. Exhib.*, **2001**, SAMPE, Long Beach, 1506-1514.

(7) McConnell, V.P., *Advanced Composites*, **1992** (May/June) p. 28.

(8) Bishop, J. *Handbook of Adhesives and Sealants*, P. Cognard (Ed.) **2005**, Elsevier, p. 319.

(9) Nair, C.P.R.; Vijayan, F.T.; Krishnan, K. *J. Appl. Polym. Sci.*, **1999**, *74*, 2737-2746.

(10) Lucintel, Global Printed Circuit Board Industry 2012-2017: Trends, Profits and Forecast Analysis, **2013**.

(11) *Polyimides*, Wilson, D.; Stenzenberger, H.D.; Hergenrother, P.M. (Eds), Blackie A&P; Glasgow, **1990**, pp. 79-128.

(12) Gaku, M.; Suzuki, K.; Ikeguchi, N. *Proc. Electr. Electron. Insul. Conf.*, **1977**, *13*, 11-14.

(13) Reference (1), pp. 230-256.

(14) Fang, T.; Shimp, D.A. *Prog. Polym. Sci.*, **1995**. *20*, 61-118.

(15) Sun, H.; Mumby, S. J.; Maple, J.R.; Hagler, A.T. *J. Am. Chem. Soc.* **1994**, *116*, 2978.

(16) Wu, H.D.; Ma, C.C.M.; Chu, P.P.; Tseng, H.T.; Lee C.T. *Polymer* **1998**, *39*, 2859-2861.

(17) Chu, P.P.; Wu, H.D. *Polymer* **2000**, *41*, 101-109.

(18) Lin, Y.; Jin, J.; Song, M.; Shaw, S.J. ; Stone, C.A. *Polymer* **2011**, *52*, 1716.

(19) Baggott, A.; Bass, J.R. ; Hall, S.A. ; Hamerton, I. ; Howlin, B.J. ; Mooring, L. ; Sparks, D. *Macromol. Theory Simul.* **2014**, *23*, 369-372.

(20) Bauer, M.; Uhlig, C.; Bauer, J.; Harris, S.; Dixon, D. Side reactions during polycyclotrimerisation of cyanates and their influence on network structure and properties, Chapter 23 in *Wiley Polymer Networks Group Review Series Volume 2*, B.T. Stokke and A. Elgsaeter (Eds.), Chichester: John Wiley, **1999**, pp. 271-283.

(21) Berendsen, H.J.C.; Postma, J.P.M.; van Gunsteren, W.F.; DiNola, A.; Haak, J.R. *J. Chem. Phys.* **1984**, *81*, 3684-3690.

(22) Crawford, A.C., *Novel Cyanate Ester Blends*, PhD Thesis, University of Surrey, **2013**.

(23) Bauer, M.; Bauer, J.; Garsk, B. *Acta Polym.*, **1986**, *37*, 604.

(24) Lin, R.H.; Hong, J.L.; Su, A.C. *Proc. Am. Chem. Soc., Div. Polym. Mat. Sci. Eng.* **1992**, *66*, 464.

(25) Khanna, Y.P.; Kumar, R.; Das, S. *Polym. Eng. Sci.* **1990**, *30*, 1171.

(26) Zeng, X.; Yu, S.; Sun, R. *J. Thermal Anal. Calor.*, **2013**, *114*, 387-395.

(27) Nair, C.P.R.; Francis, T.; Vijayan, T.M.; Krishnan, K. *J. Appl. Polym. Sci.*, **1999**, *74*, 2737–2746.

(28) Lin, R.; Lu, W.H.; Lin, C.W. *Polymer*, **2004**, *45*, 4423–4435.

(29) Liu, X.; Yu, Y.; Li, S. *Polymer*, **2006**, *47*, 3767–3773.

(30) Yan, H.Q.; Wang, H.Q.; Cheng, J. *Eur Polym J.*, **2009**, *45*, 2383–2390.

(31) Barton, J.M.; Hamerton, I.; Jones, J.R. *Polym. Internat.*, **1992**, *29*, 145-156.

(32) Barton, J.M.; Hamerton, I.; Rose, J.B.; Warner, D. *Polymer*, **1991**, *32* 358-363.

(33) Hamerton, I.; Howlin, B.J.; Klewpatinond, P.; Shortley, H.J.; Takeda, S. *Polymer*, **2006**, *47*, 690-698.

(34) Crawford A.O. ; Hamerton, I. ; Cavalli, G.; Howlin, B.J. *PLoS ONE*, **2012**, *7*, e44487.

(35) Abraham, T. *J. Polym. Sci., Part C. Polym. Lett.*, **1988**, *26*, 521-528.

(36) Chaplin, A.; Hamerton, I.; Howlin, B.J.; Barton, J.M. *Macromolecules*, **1994**, *27*, 4927–4935.

(37) Hamerton, I.; Howlin, B.J.; Jewell, S.L.; Patel, S. *React. Func. Polym.*, **2012**, *72*, 279-286.

(38) Hamerton, I.; Barton, J.M.; Chaplin, A.; Howlin, B.J.; Shaw, S.J. *Polymer*, **2001**, *42*, 2307-2319.

(39) He, Y.R.; Dai, P.B.; Xu, J.W.; Lu, Y.Q.; Wang, H. *Adv. Mater. Res.*, **2013**, *788*, 159-163.

(40) Bauer, M.; Bauer, J.; Kuhn, R. G. *Acta Polym.*, **1989**, *40*, 397-397.

(41) Hamerton, I.; Takeda, S. *Polymer*, **2000**, 41, 1647-1656.

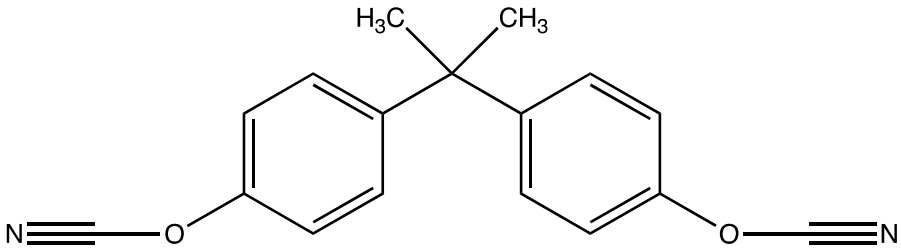

(1)

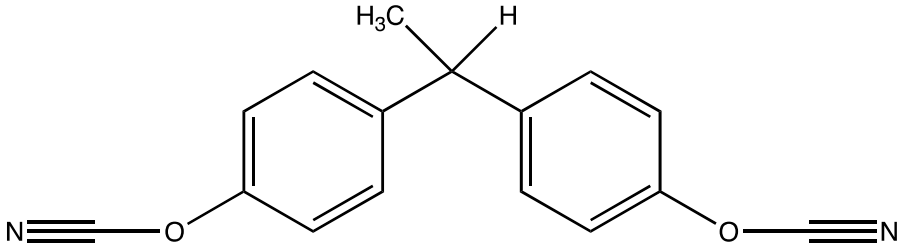

(2)

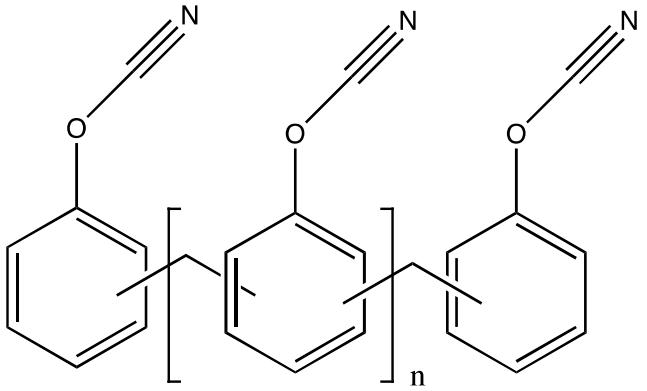

(3)

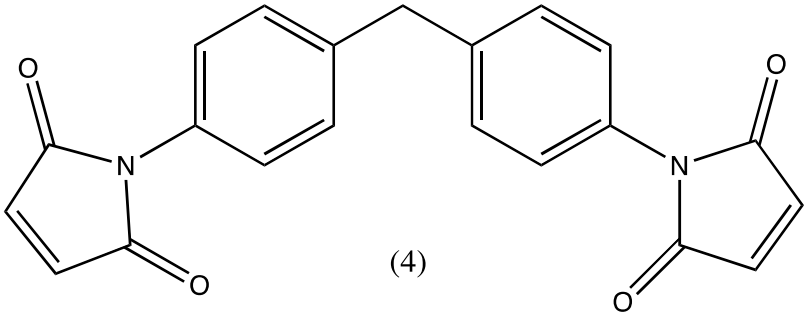

(4)

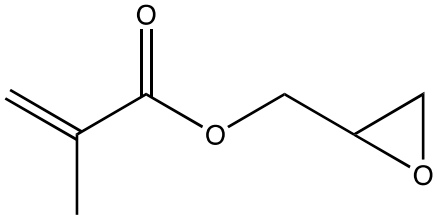

(5)

Scheme 1 Monomer structures studied in this work (*N.B.*, in this instance n = 1 in structure (3))

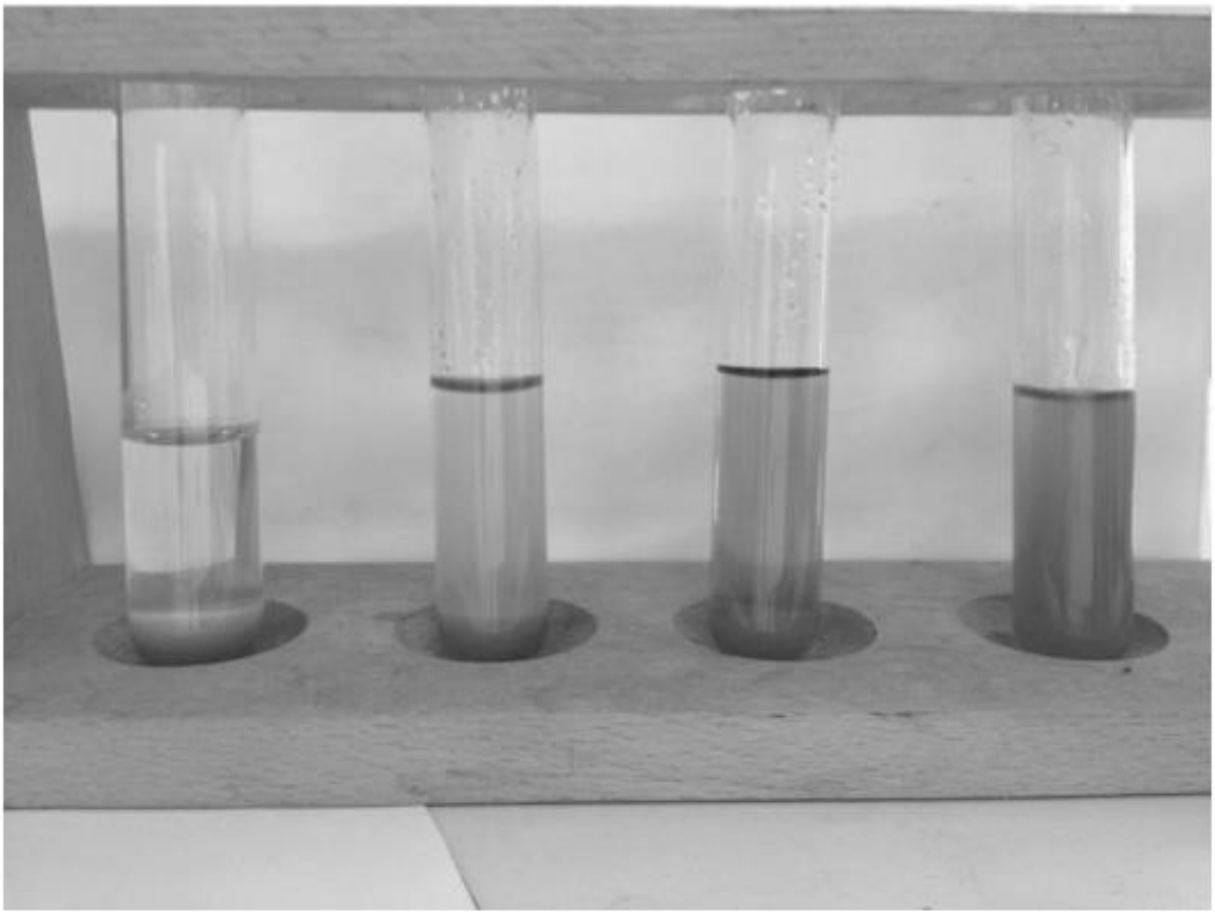

Fig. 1 Samples A-D (left to right). Note the treatment of samples E-G did not effect dissolution.

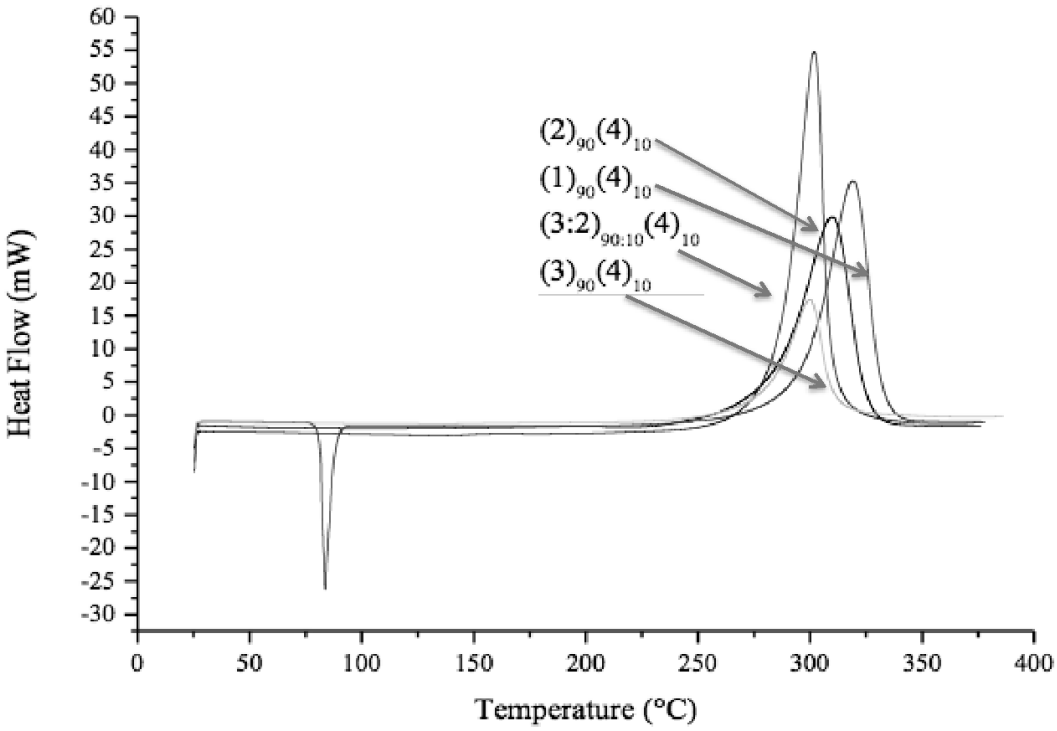

Fig. 2 DSC analysis of $(1)_{90}$-$(4)_{10}$, $(2)_{90}$-$(4)_{10}$, $(3)_{90}$-$(4)_{10}$, and $(3:2)_{90:10}$-$(4)_{10}$.

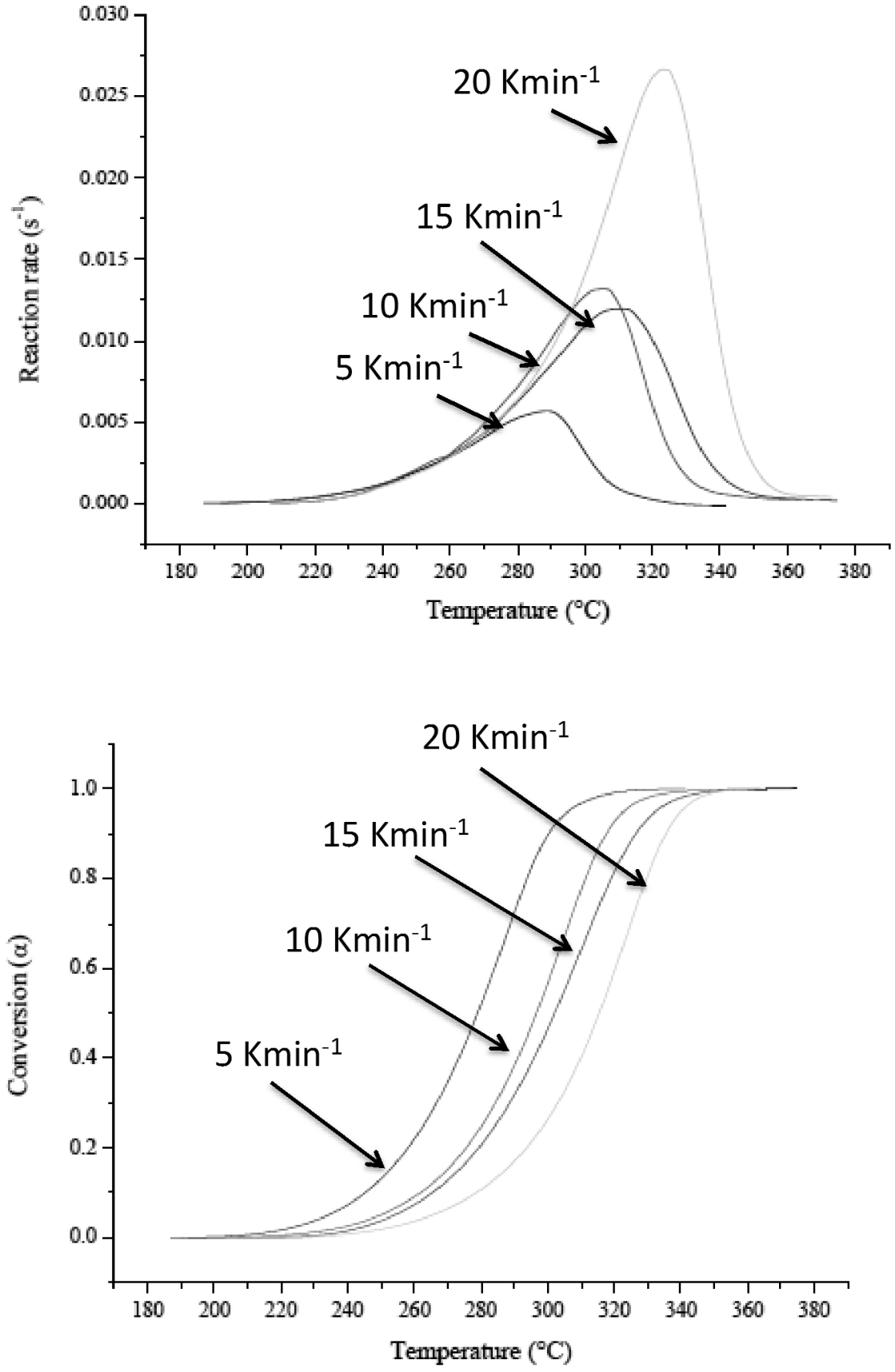

Fig 3 Plots of (a) reaction rate and (b) fractional conversion data from DSC heating scan (various heating rates, under nitrogen) for $(1)_{90}$-$(4)_{10}$.

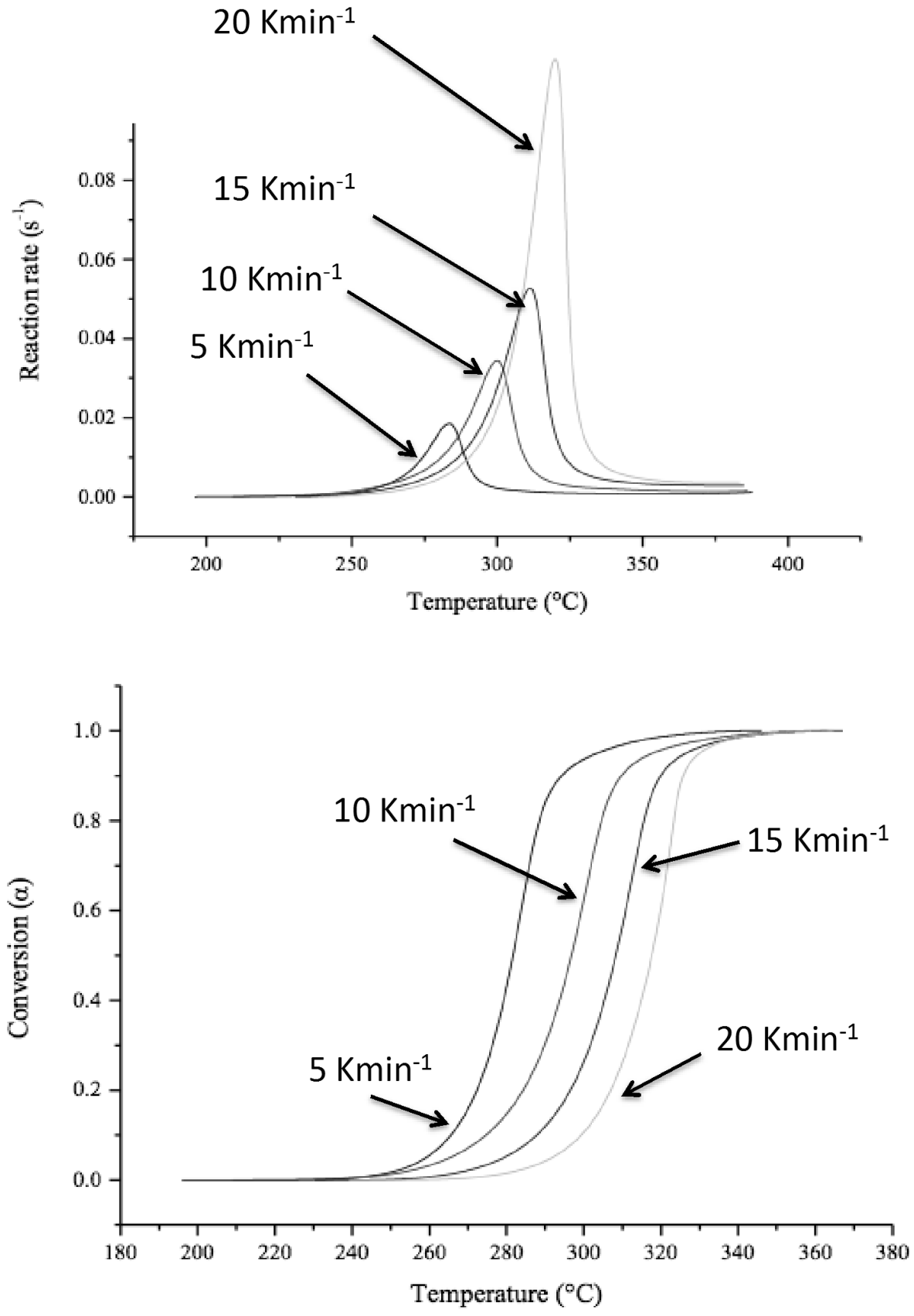

Fig 4 Plots of (a) reaction rate and (b) fractional conversion data from DSC heating scan (various heating rates, under nitrogen) for $(3)_{90}$-$(4)_{10}$.

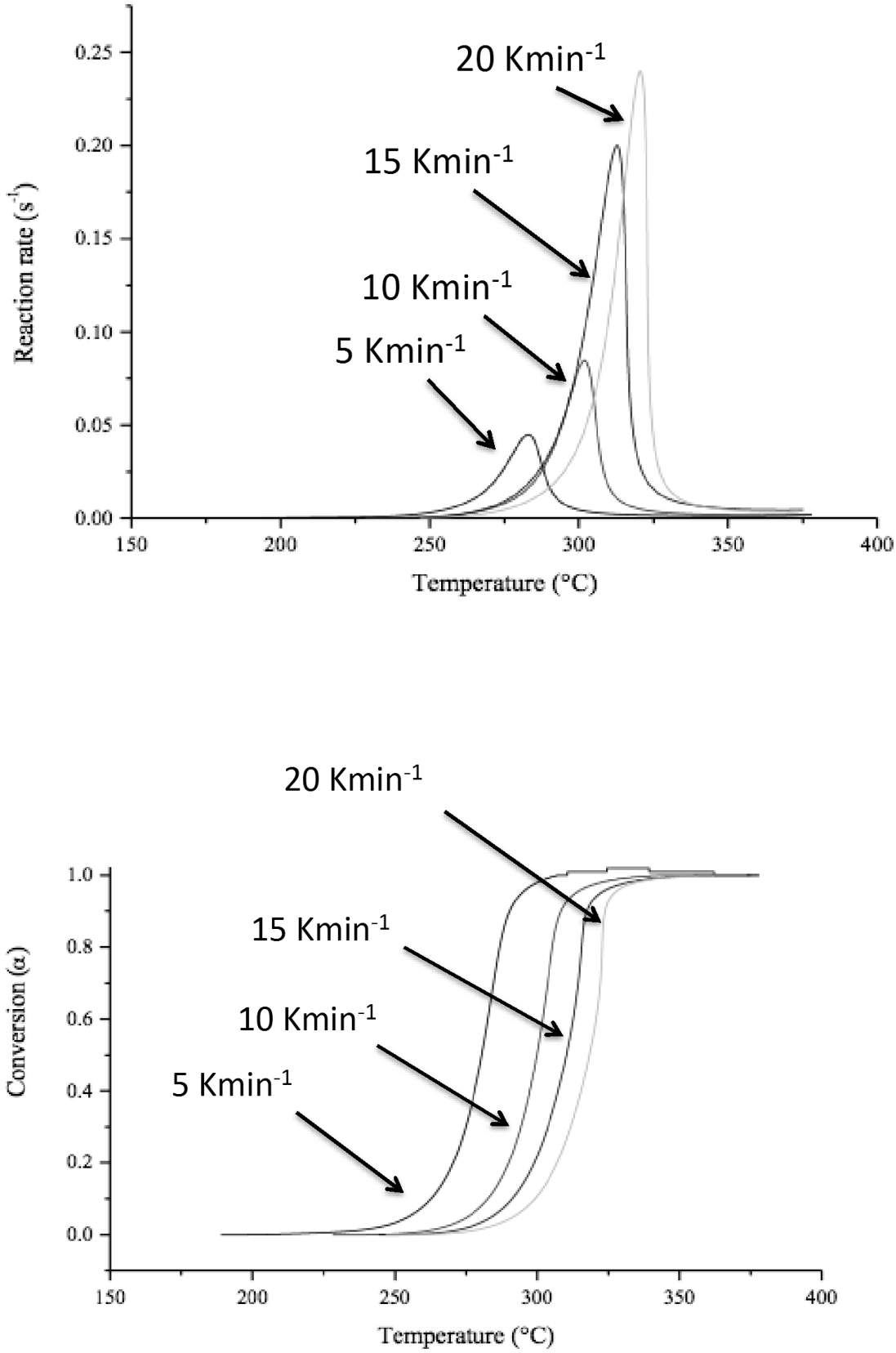

Fig 5 Plots of (a) reaction rate and (b) fractional conversion data from DSC heating scan (various heating rates, under nitrogen) for $(3{:}2)_{90:10}$-$(4)_{10}$.

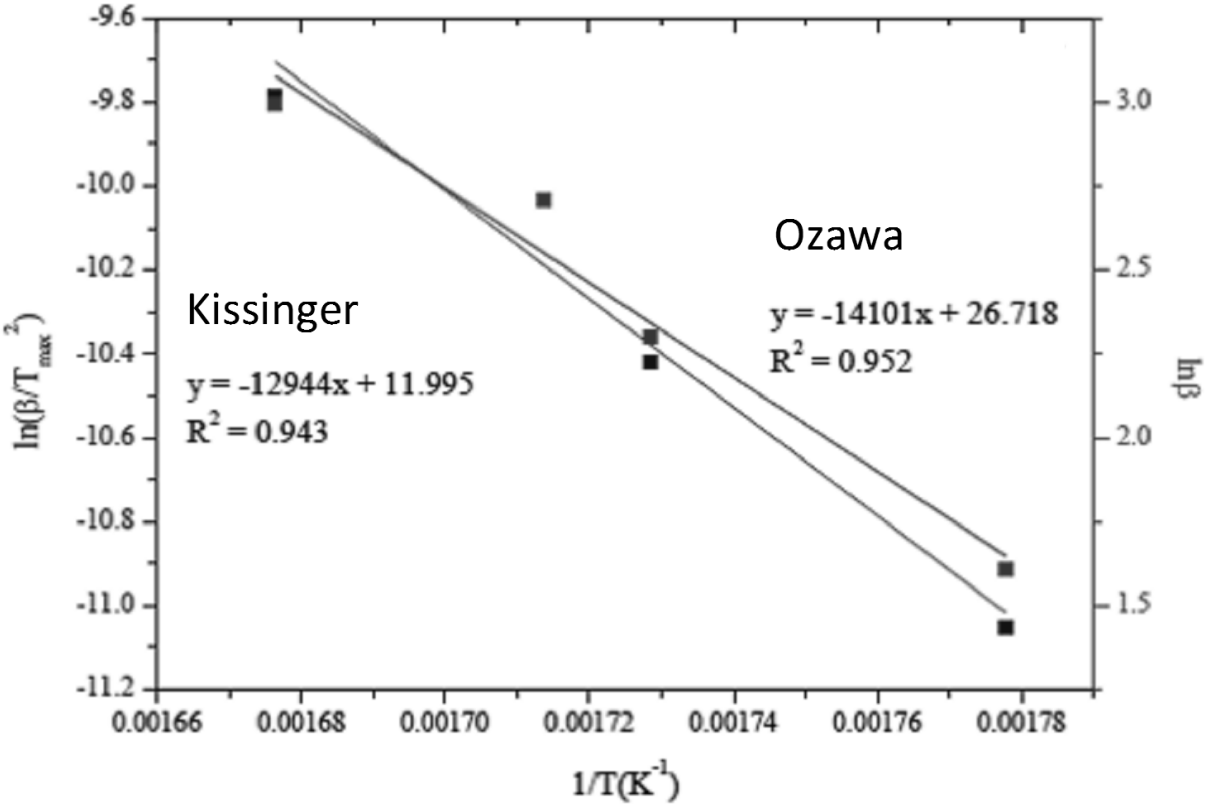

Fig. 6 Kinetic parameters from DSC heating scan (various heating rates, nitrogen) for $(1)_{90}$-$(4)_{10}$.

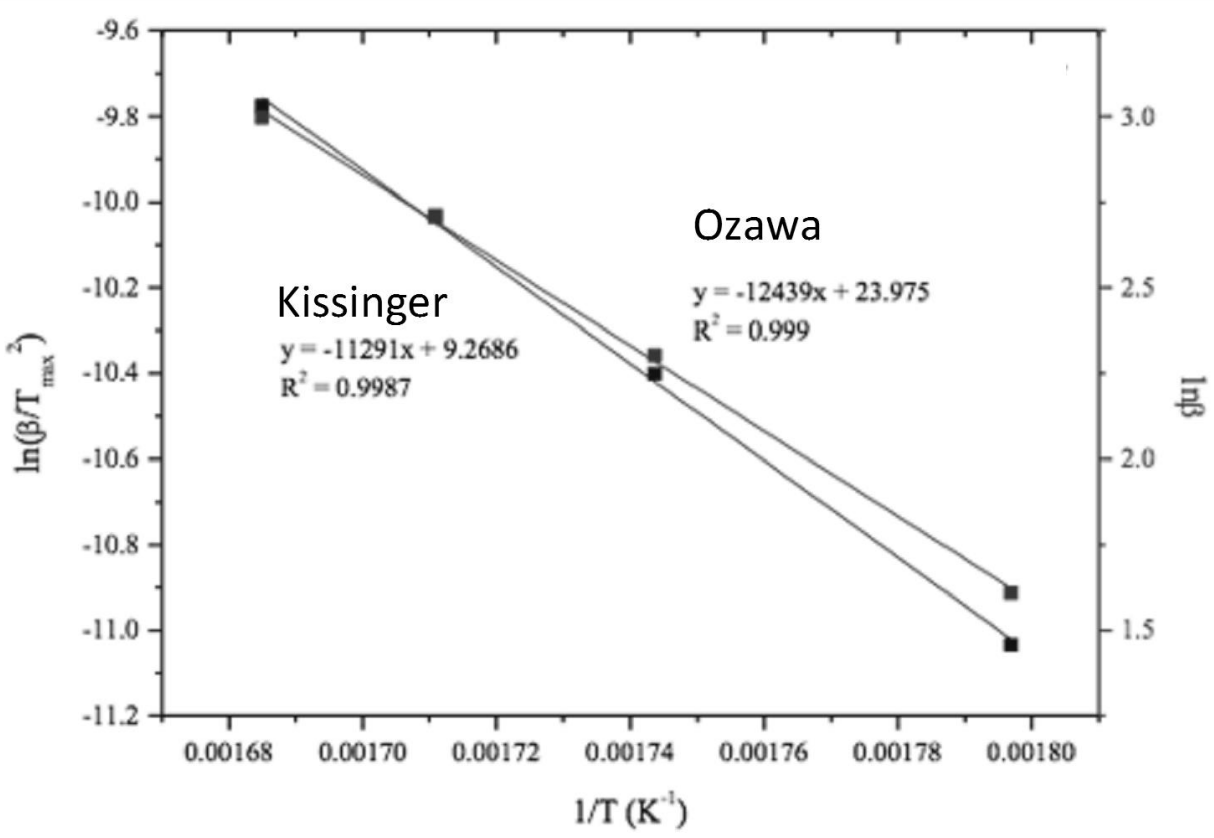

Fig. 7 Kinetic parameters from DSC (various heating rates, nitrogen) for $(3)_{90}$-$(4)_{10}$.

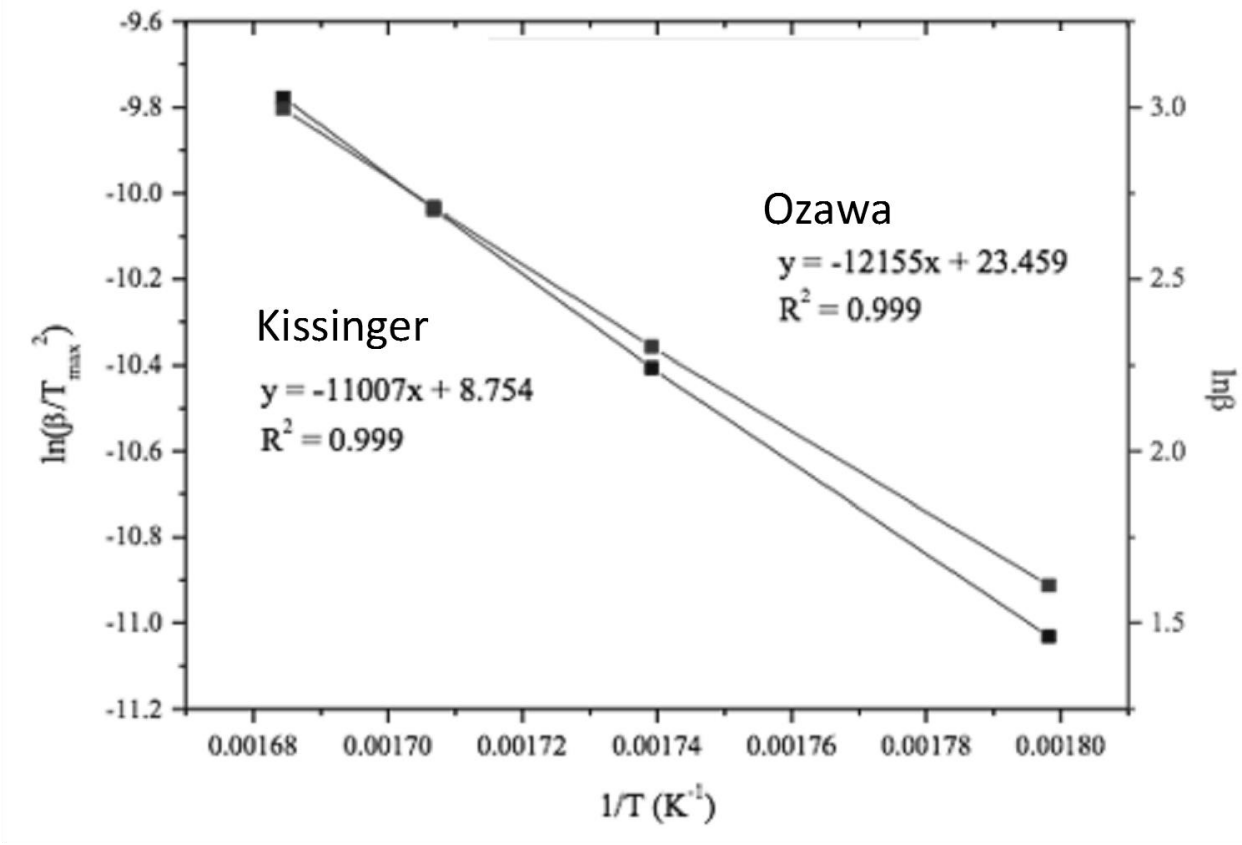

Fig. 8 Kinetic parameters from DSC (various heating rates, nitrogen) for $(3:2)_{90:10}$-$(4)_{10}$.

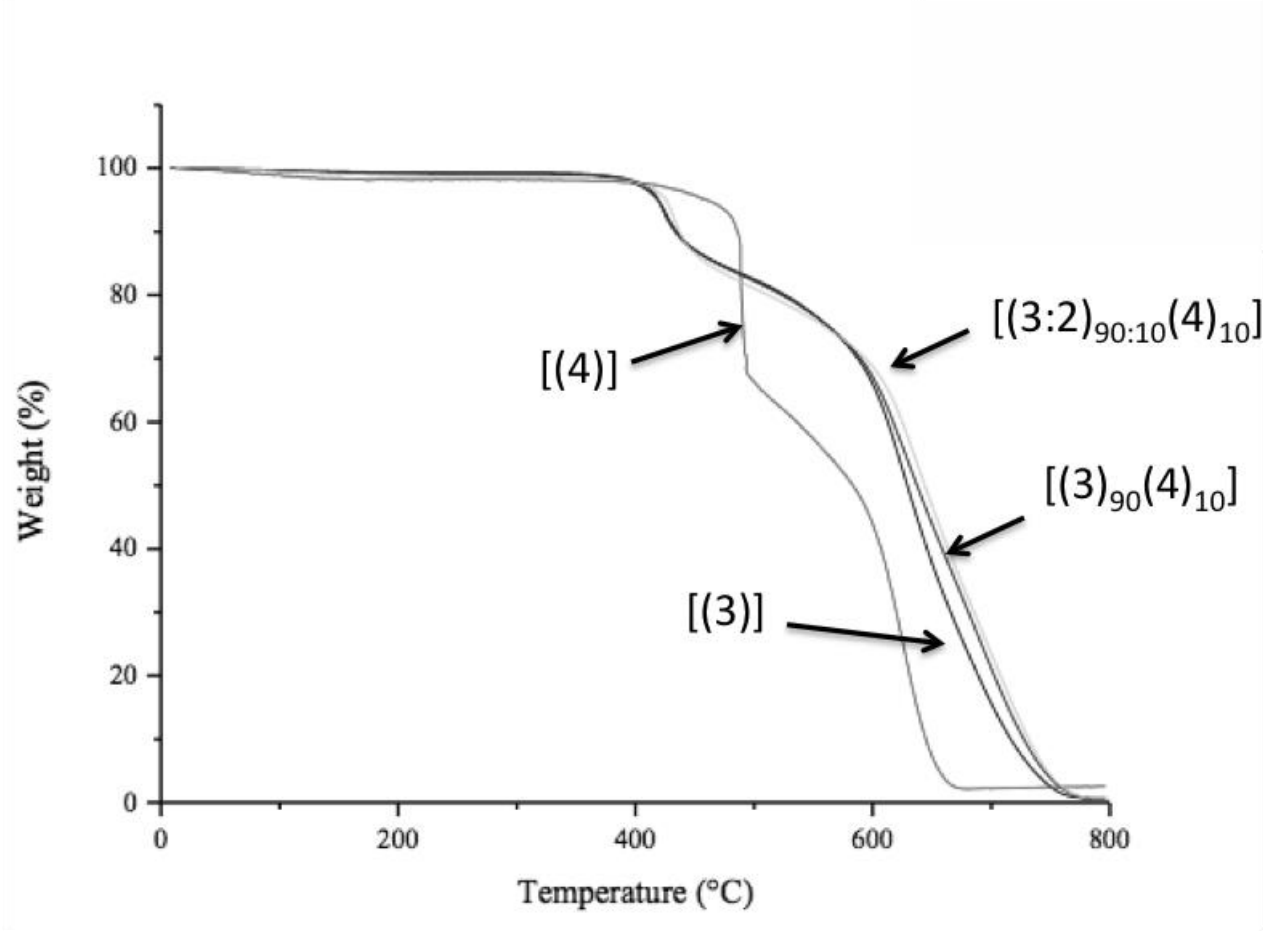

Fig. 9 Thermo-oxidative stability of the cured BT resin blends (10 K/min, static air).

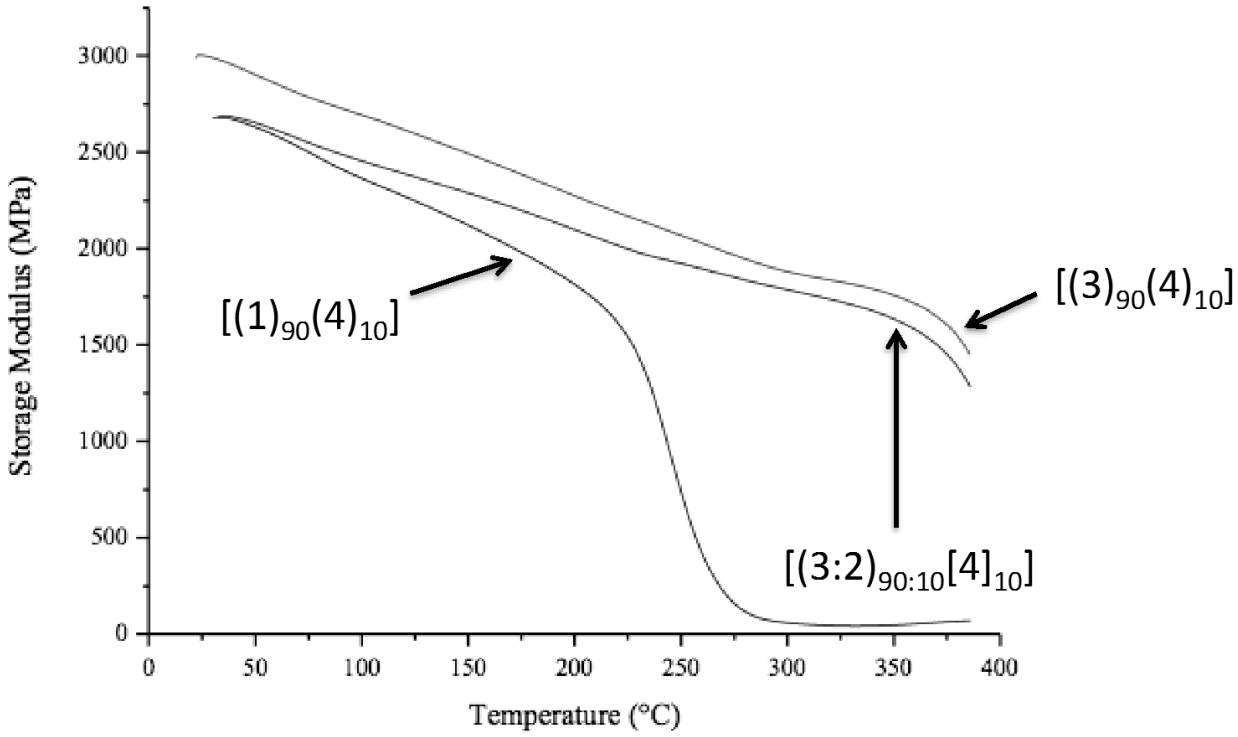

Fig. 10 Comparison of DMTA data for selected cured polycyanurate-BMI blends.

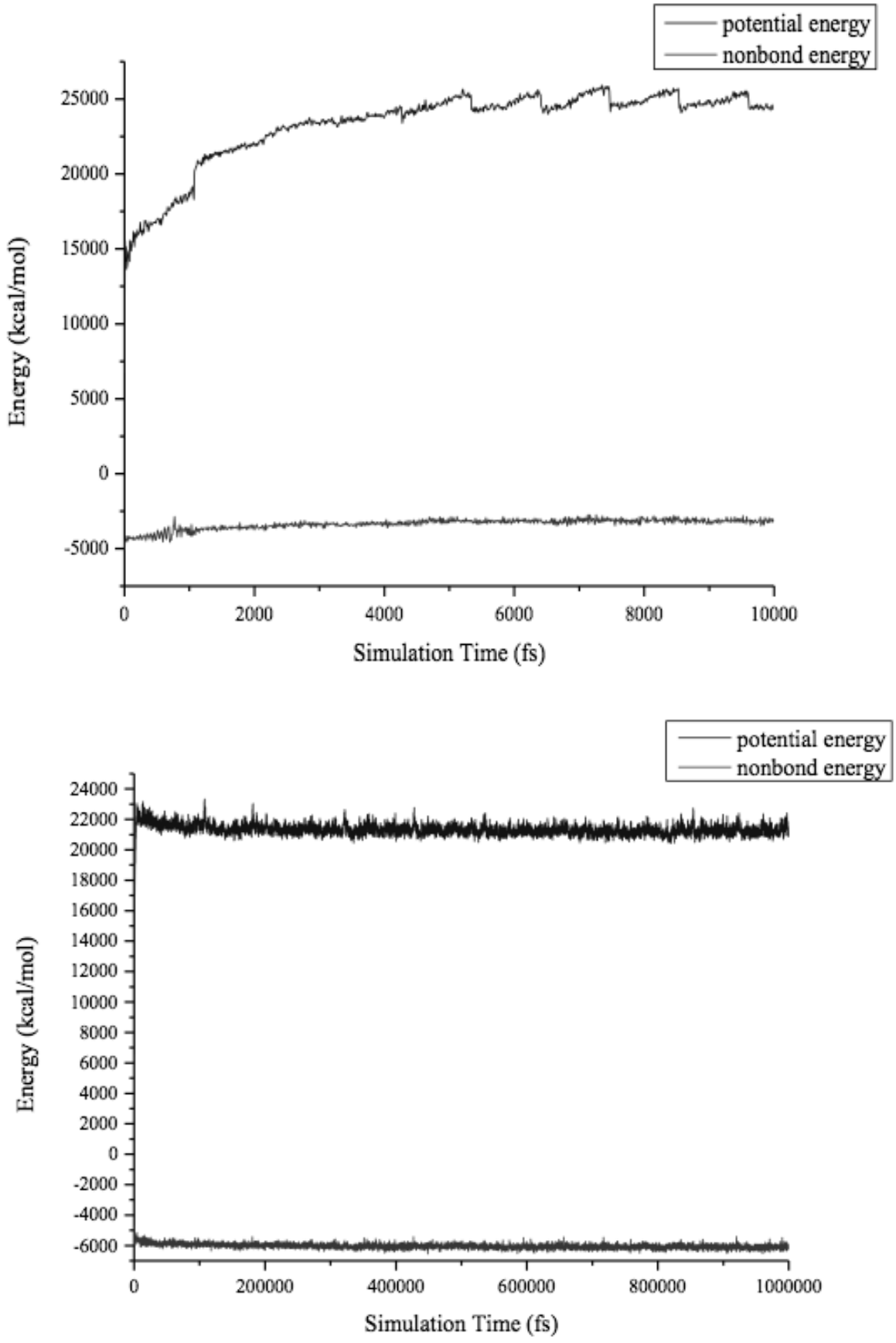

Fig. 11 MD temperature equilibration over (a) 10000 fs (10 ps), (b) 1 ns. In each case the potential energy is the upper plot, with the non bond energy below.

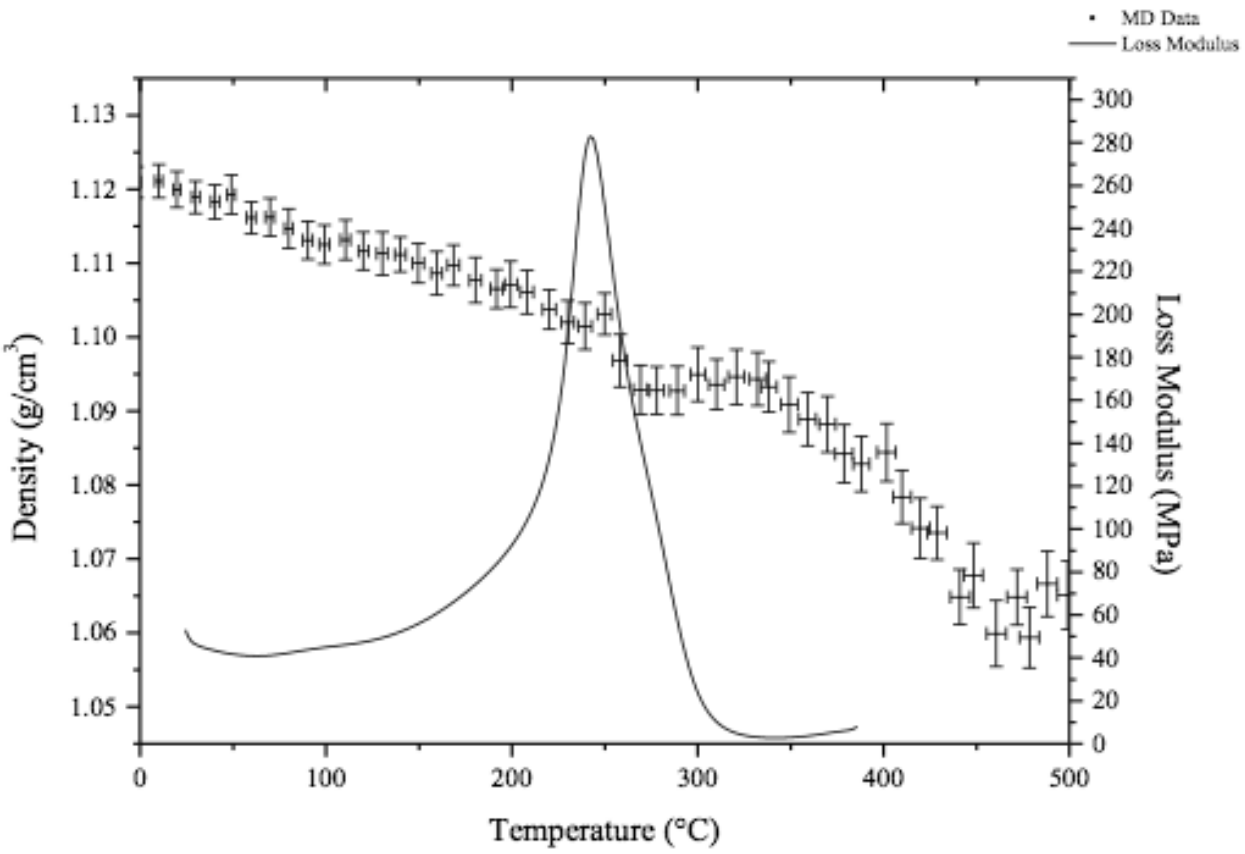

Fig. 12. MD density data for $[(1)_{90}\text{-}(4)_{10}]$ superimposed on loss modulus data (single cantilever, K/min, under nitrogen)

Table 1 Designation of monomers and composition of blends (wt %) examined in this work

Sample Designation	**Cyanate Ester**			**BMI**	**GMA**
	1	**2**	**3**	**4**	**5**
(1)	100	0	0	0	0
(2)	0	100	0	0	0
(3)	0	0	100	0	0
$(1)_{90}$-$(4)_{10}$	90	0	0	10	0
$(2)_{90}$-$(4)_{10}$	0	90	0	10	0
$(3)_{90}$-4_{10}	0	0	90	10	0
$(3)_{80}$-$(4)_{20}$	0	0	80	20	0
$(3)_{70}$-$(4)_{30}$	0	0	70	30	0
$(3)_{60}$-$(4)_{40}$	0	0	60	40	0
$(3)_{50}$-$(4)_{50}$	0	0	50	50	0
$(3:2)_{90:10}$-$(4)_{10}$	0	10	90	10	0
$(1:4)_{90:10}$-$(5)_{2.5}$	90	0	0	10	2.5
$(1:4)_{90:10}$-$(5)_{5}$	90	0	0	10	5
$(1:4)_{90:10}$-$(5)_{10}$	90	0	0	10	10

Key the composition of the blend is indicated by the subscript. Thus, a blend comprising 90 wt % of monomer (1) and 10 wt % of monomer (4) is denoted $(1)_{90}$-$(4)_{10}$. Cured blends are denoted by the use of square brackets to differentiate them from the corresponding monomer blend *i.e.* monomer blend $(1)_{90}$-$(4)_{10}$ becomes polycyanurate $[(1)_{90}$-$(4)_{10}]$ following cure.

Table 2 Conditions applied to aid co-solvation of (2) and (4).

Sample Designation	Conditions	Temperature	Frequency/speed	Duration
A	No agitation	RT	-	1 week
B	Sonication	RT	35 kHz	15 mins
C	Sonication	RT	35 kHz	20 mins
D	Sonication	50	35 kHz	30 mins
E	Stirring	50	300 rpm	30 mins
F	Stirring	50	300 rpm	60 mins
G	Stirring	RT	300 rpm	3 days

Table 3 DSC data for uncured novel bismaleimide-triazine blends (nitrogen, 10 K/minute)

Material	T_o (°C)	T_{max} (°C)	Polymerisation enthalpy, ΔH_p (J/g)
$(1)_{90}$-$(4)_{10}$	217	319	707
$(2)_{90}$-$(4)_{10}$	218	309	746
$(3)_{90}$-$(4)_{10}$	195	300	573
$(3:2)_{90:10}$-$(4)_{10}$	189	302	696

Key: T_o = onset of polymerization exotherm, T_{max} = peak maximum of polymerization enthalpy, ΔH_p = Enthalpy of polymerization.

Table 4 Kinetic parameters (DSC data) for uncured novel bismaleimide-triazine blends

Sample	Activation energy		RMSE		Reaction rate (s^{-1})
	Kissinger	Ozawa	Kissinger	Ozawa	
$(1)_{90}$-$(4)_{10}$	107.62	111.45	0.04	0.04	0.212
$(3)_{90}$-$(4)_{10}$	93-98	98.31	0.01	0.01	0.185
$(3:2)_{90:10}$-$(4)_{10}$	90.68	105.44	0.01	0.01	0.175

Table 5 Thermo-oxidative stability data (10 $Kmin^{-1}$, static air) for cured homopolymers and binary cyanate ester blends as determined by TGA

Sample	**Temperature (°C) for mass loss**							
	5 %	10 %	20 %	30 %	40 %	50 %	60 %	70 %
[(1)]	413	423	428	435	458	538	575	590
[(2)]	417	422	430	452	530	571	588	600
[(3)]	419	435	526	587	613	629	646	666
[(4)]	460	486	488	493	536	583	607	620
$[(1)_{90}\text{-}(4)_{10}]$	400	410	430	440	500	560	595	610
$[(3)_{90}\text{-}(4)_{10}]$	419	434	524	590	617	638	659	681
$[(3)_{80}\text{-}(4)_{20}]$	417	430	510	574	609	629	645	665
$[(3)_{70}\text{-}(4)_{30}]$	414	427	491	571	607	626	644	664
$[(3)_{60}\text{-}(4)_{40}]$	414	428	509	576	605	620	635	652
$[(3)_{50}\text{-}(4)_{50}]$	423	438	468	550	603	621	635	649
$[(3{:}2)_{90:10}\text{-}(4)_{10}]$	425	440	529	590	623	641	662	684

Table 6 Storage moduli (DMTA) for cured homopolymers and blends.

Sample	Storage modulus (MPa)	
	at 30 °C	at 300 °C
[(1)]	2782	< 100
[(2)]	2704	< 100
[(3)]	3294	2200
$[(1)_{90}\text{-}(4)_{10}]$	2700	< 100
$[(3)_{90}\text{-}(4)_{10}]$	2990	1800
$[(3)_{80}\text{-}(4)_{20}]$	3220	1964
$[(3)_{70}\text{-}(4)_{30}]$	3271	2018
$[(3)_{60}\text{-}(4)_{40}]$	3274	2002
$[(3{:}2)_{90:10}\text{-}(4)_{10}]$	2700	2000

N.B., cured samples of both [(4)] and $[(3)_{50}\text{-}(4)_{50}]$ were too brittle to be prepared for satisfactory analysis through DMTA.

Table 7 Effect of GMA on thermo-mechanical performance of selected blends and LIPNs

Blend	GMA (wt %)	T_g (°C)	T_d (°C)
$[(1)_{90}\text{-}(4)_{10}]$	0	300	406
$[(1{:}4)_{90:10}\text{-}(5)_{2.5}]$	2.5	275	397
$[(1{:}4)_{90:10}\text{-}(5)_{5}]$	5	267	397
$[(1{:}4)_{90:10}\text{-}(5)_{10}]$	10	274	386

Key:

T_g = glass transition temperature (measured as peak maximum in loss modulus at 10 K/min under nitrogen).

T_d = onset of thermo-oxidative degradation equating to 5 % weight loss (measured at 10 K/min in static air).